PAPER *Special Section on Recent Progress in Electromagnetic Theory and Its Application*

Design and Fabrication of a Metasurface for Bandwidth Enhancement of RCS Reduction Based on Scattering Cancellation

Hiroshi SUENOBU[†a], **Shin-ichi YAMAMOTO**[†], **Michio TAKIKAWA**[††], *and* **Naofumi YONEDA**[†], ***Members***

SUMMARY A method for bandwidth enhancement of radar cross section (RCS) reduction by metasurfaces was studied. Scattering cancellation is one of common methods for reducing RCS of target scatterers. It occurs when the wave scattered by the target scatterer and the wave scattered by the canceling scatterer are the same amplitude and opposite phase. Since bandwidth of scattering cancellation is usually narrow, we proposed the bandwidth enhancement method using metasurfaces, which can control the frequency dependence of the scattering phase. We designed and fabricated a metasurface composed of a patch array on a grounded dielectric substrate. Numerical and experimental evaluations confirmed that the metasurface enhances the bandwidth of 10dB RCS reduction by 52% bandwidth ratio of the metasurface from 34% bandwidth ratio of metallic cancelling scatterers.
key words: *radar cross section (RCS), metasurface, scattering cancelletion, periodic structure, equivalent circuit design*

1. Introduction

Metasurfaces controlling reflection characteristics through their periodic structure have been developed in recent years. Metasurfaces are a type of two-dimensional surface-structured metamaterials. The metamaterials realize properties that are nothing in nature through periodic structures of metals, dielectrics, and other materials.

One of usages of metamaterials is radar cross section (RCS) reduction, which reduce scattered waves from scatterers. RCS reduction using metamaterials has been focused on since cloaking, which detours incident waves around a target, was realized using a structure with a negative refractive index [1], [2]. However, the applicability of cloaking is restricted because it requires a complex three-dimensional structure and narrow-band resonance phenomena. Subsequently, mantle-cloak was proposed in which metamaterials cover the target scatterer as a thin surface structure to suppress scattering waves [3]. A typical example of mantle-cloak uses scattering cancellation. It was realized by the scattered waves from a two-dimensional periodic structure and the scattered waves from the back side of the structure to be the opposite phase, and then the waves cancel each other [4].

Scattering cancellation is a common method of RCS reduction and can be done by putting a canceling scatterer (hereafter referred to as a canceller) in the neighborhood of the target scatterer. If the canceller consists of metallic material, the cancellation occurs only at frequencies where the distance between the target scatterer and the canceller becomes around 1/4 wavelength, where the phase difference between them becomes around 180°. Mantle-cloak made it possible to cause scattering cancellation with a distance much less than 1/4 wavelength by controlling the reflection phase through its periodic structure. Metamaterials with such thin two-dimensional structures are now generally called metasurfaces [5].

In the case of the mantle-cloak, the attempt initially focused on obtaining thinner structures. Thus its bandwidth was still narrow. On the other hand, checkerboard metasurfaces were proposed as a structure that can significantly expand the bandwidth of scattering cancellation [6]. The checkerboard metasurfaces are composed of a combination of more than two parts of the surface, at least one of which acts as AMC (Artificial Magnetic Conductor) [7]. The form of the checkerboard metasurfaces looks like chessboards. In particular, a checkerboard structure consisting of two types of metasurfaces with their reflection phase frequency characteristics being different by 180°over a broad bandwidth realizes broadband RCS reduction by causing scattering cancellation over the broad bandwidth [8]. Further bandwidth extension has been developed by using a variety of element types in the periodic structure [9] or by increasing the number of partial surfaces consisted different types of elements [10], [11]. Expansion of the angular coverage of the reduction has also been developed by optimizing element placement [12]–[14] and by using elements with a three-dimensional structure [15], [16].

However, these kinds of metasurfaces cannot be available when they cannot be mounted directly on the target since they may obstruct the original function of the target. For example, by mounting a metasurface on an antenna's aperture, the antenna's original function might not work because the metasurface blocks the wave emitted from the aperture. Some studies have been conducted on antennas to achieve both RCS reduction and antenna function [17]–[20], but issues remain to be addressed. Active cancellation can also be considered as a method based on scattering cancellation that avoids direct mounting on the target [21]–[24]. The active cancellation works by receiving the incident wave and retransmitting it with adjustment to be the same amplitude and opposite phase against to the incident wave. This mechanism requires complex active systems; thus, active cancellation is

Manuscript received April 9, 2023.
Manuscript revised July 22, 2023.
Manuscript publicized September 19, 2023.
[†]The authors are with Mitsubishi Electric Corporation, Kamakura-shi, 247–8501 Japan.
[††]The author is with Mitsubishi Electric Corporation, Tokyo, 100–8310 Japan.
a) E-mail: Suenobu.Hiroshi@ab.MitsubishiElectric.co.jp
DOI: 10.1587/transele.2023REP0002

hard to implement in a realistic situation.

In this paper, we propose and study a method of expanding the bandwidth of RCS reduction by putting a metasurface around the target. In this method, we can avoid obstructions to the target's original functions by putting it sufficiently away from the target where an electrical coupling between the target and the metasurface is sufficiently small. The metasurface can control its reflection phase on broader frequencies, where cancellation causes than metallic scatterers. It could be a method for bandwidth enhancement of RCS reduction without any system complexity and obstruction on the target function. We select that an actual structure of the metasurface is a patch array on a substrate, and we design it using an equivalent circuit model and fabricate a sample. Electromagnetic simulations and measurements of the fabricated sample verify the effectiveness of the design.

The structure of this paper is as follows: Sect. 2 describes the RCS reduction method based on scattering cancellation and the design method of the metasurface, Sect. 3 describes design results and evaluations by electromagnetic simulations, Sect. 4 shows evaluation results by fabrication and measurements, finally, Sect. 5 presents the conclusion.

2. Method for Reducing RCS and Design

This section shows the method for reducing RCS using the metasurface and design.

2.1 Method for Deducing RCS by Scattering Cancellation

The method for reducing RCS by scattering cancellation is schematically shown in Fig. 1. The canceller, which has the same scattered field magnitude (hereafter referred to as an amplitude) as the target, is placed on nearby the target with distance δ. Taking the amplitude of the target $\mathrm{A_t}$, the complex reflection coefficient Γ_t, the amplitude of the canceller $\mathrm{A_c}$, its complex reflection coefficient Γ_c, the superposition of target and canceller waves S is expressed as

$$S = \mathrm{A_t}\Gamma_\mathrm{t} + \mathrm{A_c}\Gamma_\mathrm{c}\exp(2jk_0\delta), \tag{1}$$

where k_0 is the wave number in the vacuum. We define an amount of the scattered amplitude reduction as

$$R_S = 20\log_{10}\left(\frac{|S|}{|\mathrm{A_t}|}\right). \tag{2}$$

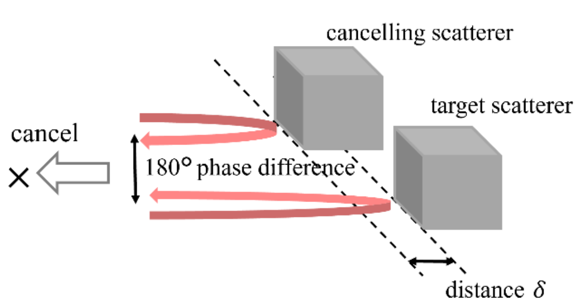

Fig. 1 RCS reduction by scattering cancellation.

This quantity corresponds to the reduction of RCS. If the target and the canceller give the same amplitudes, the reduction is maximized when the distance δ is $\lambda/4$, where λ is the wavelength in the vacuum. We set a typical criterion for reduction of RCS 10dB. The condition for obtaining 10dB reduction is that phase difference between the target wave and the canceller wave is in a range $180^\circ \pm 15^\circ$ and this corresponds to 20% bandwidth ratio for the metallic canceller case.

2.2 Bandwidth Enhancement by Metasurface

Bandwidth enhancement of scattering cancellation by metasurfaces is discussed below. This work considers a metasurface composed of a metallic patch array on a grounded dielectric substrate, and this structure is shown in Fig. 2. An equivalent circuit model of this patch array is well known as Fig. 3 [25], [26].

Considering a case of normal incidence, an input impedance of the patch array is given by [27]

$$Z_\mathrm{in} = \frac{j\omega\mu_0\frac{\tan(kd)}{k}}{1-2k_\mathrm{eff}\alpha\frac{\tan(kd)}{k}}, \tag{3}$$

$$\alpha = \frac{k_\mathrm{eff}\mathrm{D}}{\pi}\ln\left(\frac{1}{\sin\frac{\pi w}{2D}}\right) \tag{4}$$

where ω is the angular frequency of the incident wave, μ_0 is the permeability of the free space, k is the wavenumber in

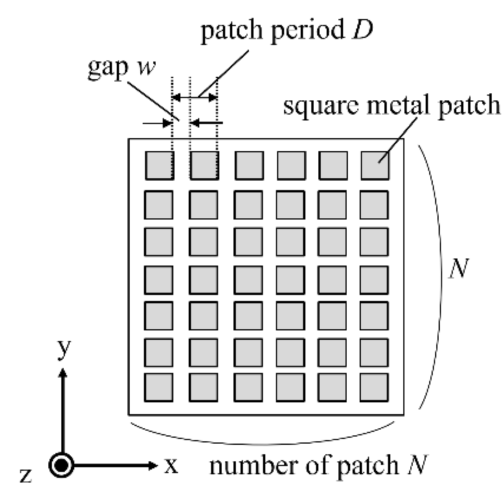

(a) top view

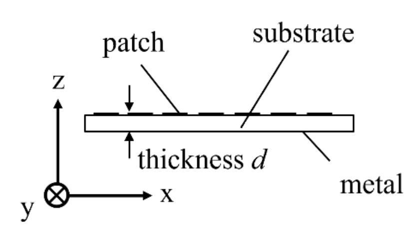

(b) side view

Fig. 2 Metasurface composed of the patch array.

the substrate with relative permittivity ε_r, k_{eff} is an effective wavenumber around the boundary between the free space and the substrate and given by $k_{\mathrm{eff}} = k_0\sqrt{\varepsilon_{eff}}$ and $\varepsilon_{eff} = (1+\varepsilon_r)/2$. D is the period of the patches, w is the gap between one patch to the other, d is the thickness of the substrate. A complex reflection coefficient Γ_c of a surface with the input impedance Z_{in} is given by

$$\Gamma_\mathrm{c} = \frac{Z_{\mathrm{in}} - Z_0}{Z_{\mathrm{in}} + Z_0}, \tag{5}$$

where Z_0 is the wave impedance in the vacuum, approximately 377Ω. The efficiency of RCS reduction is evaluated by inserting Γ_c as Eq. (5) into Eq. (2).

2.3 Target Adjustment

We consider a metallic sphere the target scatterer and a flat square metasurface the canceller. We selected the sphere and the flat square because these scatterers are standard shapes, and their scattering properties are well-known analytically. For this case, the scatterer amplitude and the canceller amplitude are given by Eq. (6) [27] and Eq. (7) [28].

$$A_t = \left| \frac{\lambda}{2\sqrt{\pi}} \sum_{n=-\infty}^{\infty} \frac{(-1)^n(2n+1)}{\hat{H}_n^{(2)}(k_0\phi/2)\hat{H}_n^{(2)\prime}(k_0\phi/2)} \right| \tag{6}$$

$$A_c = \sqrt{\frac{4\pi a^4}{\lambda^2}} \tag{7}$$

Here, ϕ is the diameter of the metallic sphere (A3), a is the square's edge length, $\hat{H}_n^{(2)}$ is the spherical Hankel function of the second kind. We set the diameter of the target sphere $\phi = 8.5\lambda_c$, where λ_c is the wavelength in the center of design frequency, and then try to find a set of design parameters maximizing the bandwidth ratio of RCS reduction R_S. A determination of amplitudes of the target and the canceller are shown in Fig. 4. The horizontal axis means the normalized frequency by the center of design frequency f_c, and the vertical axis means the normalized RCS by the value on the f_c. Amplitudes are selected to be the same at the center of design frequency for the target and the canceller.

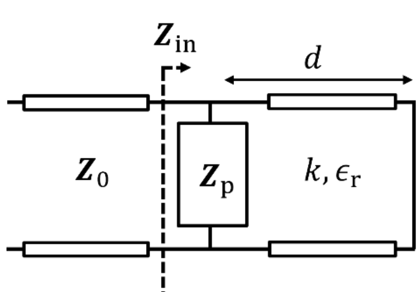

Fig. 3 Equivalent circuit model of the patch array.

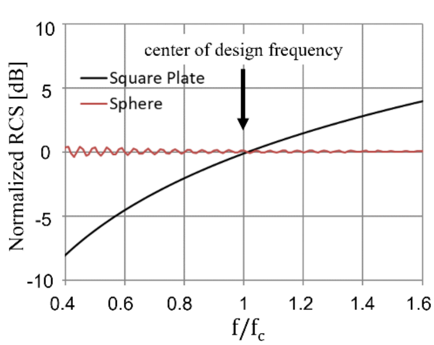

Fig. 4 Amplitude selection of scatterers.

3. Design Result

This section describes the results of the design. The determination steps of the design are the following steps—step 1. Select a material used in fabrication and set a corresponding material parameter. In this work, we use FR4 substrates, set the substrate's relative permittivity, and ignore the dielectric loss—step 2. Select the edge length of the canceller by target adjustment—step 3. Select D, w, d, N, and δ by the equivalent circuit calculation to maximize the RCS reduction bandwidth—step 4. Adjust the selected parameters by numerical simulation. In this work, we tuned only δ (details are mentioned later). We can use some optimization techniques to obtain optimal parameters throughout iterative calculations and simulations in steps 3 and 4, but we could do it by hand in this work. The resulting set of parameters is shown in Table 1.

Figure 5 shows phase characteristics of the designed metasurface obtained by electromagnetic simulations (with ANSYS HFSS). Figure 5 (a) shows RCS phase characteristics on normalized frequency. The solid black line means values obtained in the circuit model, and the solid red line means values obtained in the simulation corresponding to the same set of parameters as the circuit model (step 3). There is a discrepancy between the circuit model design and the simulation values, and this is because the period of the simulation model is finite, although the circuit model assumed infinite periodicity. The size of the metasurface is near the design wavelength. Thus, the finite periodicity could affect ideal characteristics given by the infinite periodic structure. However, we can compensate for this discrepancy by choosing distance δ in Table 1 (step 4). Figure 5 (b) shows the phase difference between the target and the designed metasurface with the distance δ obtained in the simulation. The blue line means the case of the metallic plate as the canceller, and the red line means the case of the designed metasurface as the canceller. In the case of the metasurface, the phase difference stays around 180° for the broader frequency band than the metallic case. A bandwidth ratio of the phase

Table 1 Resut of design prameters.

Parameter	Value
D	$0.083\lambda_c$
w	$0.013\lambda_c$
d	$0.043\lambda_c$
a	$1.4\lambda_c$
N	17
δ	$4.443\lambda_c$

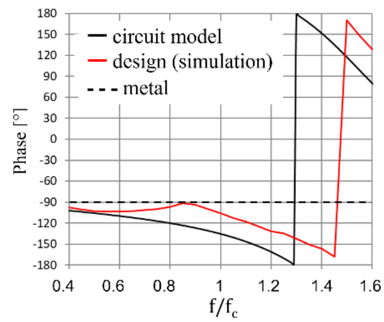

(a) Reflection phase

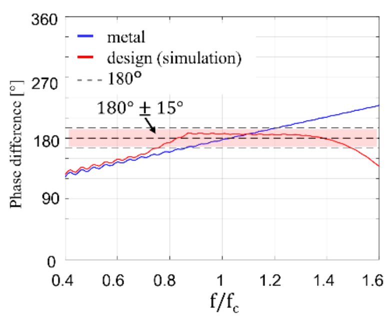

(b) Phase difference

Fig. 5 Phase characteristics of the deigned metasurface.

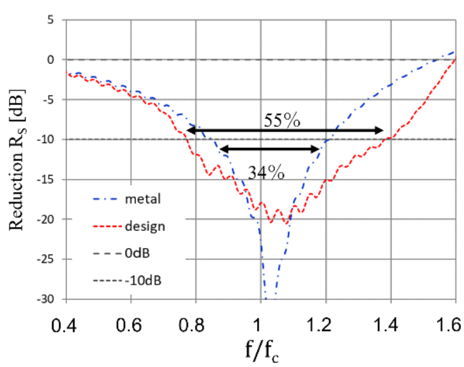

Fig. 6 RCS reduction in design

difference being within the range 180° ± 15° is 55% for the metasurface and 34% for the metallic canceller. Figure 6 shows the RCS reduction of the designed metasurface and the metallic canceller. The designed metasurface enhances 10 dB reduction bandwidth 1.6 times (34% to 55%) as the metallic canceller.

4. Fabrication and Measurement Results

In this section, we report the results of fabrication and measurements. A fabricated metasurface is shown in Fig. 7. The fabricated sample is composed of FR4 substrate with the copper patch array on the front side and the grounded back side structure.

We performed experimental evaluations on the fabricated sample by RCS measurement. A view of the

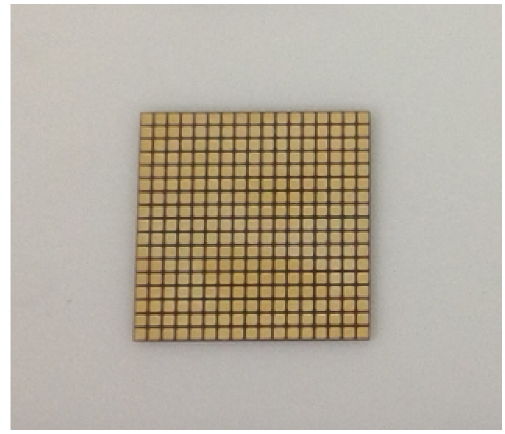

Fig. 7 Fabricated sample of the metasurface.

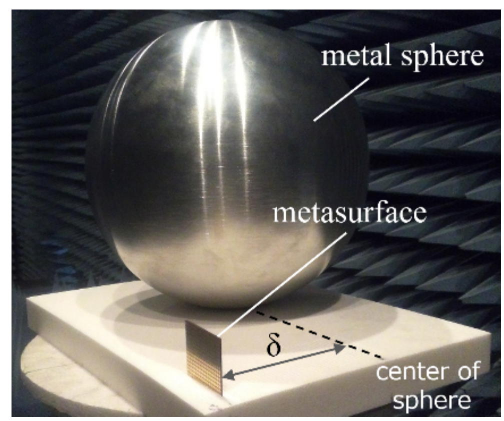

Fig. 8 View of measurement

measurement is shown in Fig. 8. The measurement was operated in the same frequency range and direction, normal to the metasurface, as in the design.

First, we measured the RCS of the fabricated metasurface alone. Figure 9 shows the results. The amplitude of the measured metasurface (the solid red line) corresponds to its simulation (the dashed red line) but is slightly different on the high-frequency side. This difference can be thought of as the effect of the dielectric loss of the substrate, which is ignored in our design. However, this difference does not bring a critical problem in this consideration because the amplitude is sufficiently close to the amplitude of the target. Thus, cancellation could work well. The RCS phase of the measured metasurface (the solid red line) also corresponds to its simulation (the dashed red line) in the range where we consider cancellation.

Then, we measured the RCS of the system consisting of the metallic sphere and the fabricated metasurface placed with the distance δ along the direction of incidence shown in Fig. 8. Figure 10 shows the results of measured RCS reduction. The horizontal axis is the normalized frequency, and the vertical axis is the RCS reduction R_s. The dashed blue line means the metallic canceller in design. The dashed red line means the metasurface in design. The solid black line

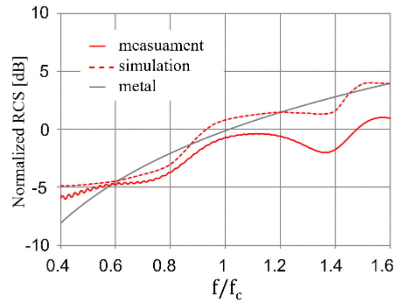

(a) Amplitude

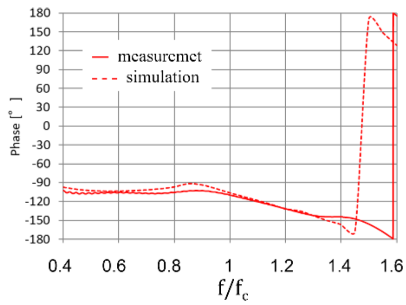

(b) Phase

Fig. 9 Measured RCS of the fabricated metasurface.

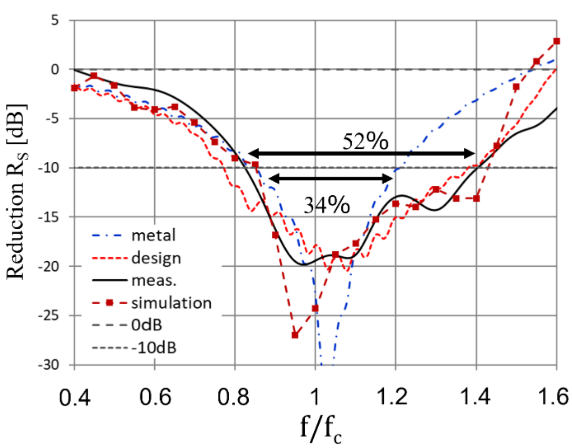

Fig. 10 RCS reduction in measurement

means measured values for the fabricated metasurface. The dashed red line with markers means a simulation result for the system composed of the sphere and the metasurface placed with the distance δ obtained by a hybrid FE-BI solver in ANSYS HFSS [29], [30]. The designed and measured values of the metasurface are in good agreement. The bandwidth ratio of 10dB reduction is enhanced by 52% of the measured metasurface from 34% of the metallic canceller in design. The effect of bandwidth enhancement by the metasurface was confirmed experimentally.

The scattering cancelation technique can be thought sensitive to alignments of measurements and fabrication errors. We checked that a directional change in the amplitude and phase of the fabricated metasurface is not so much because the size of the metasurface is around the wavelength; therefore, its scattering pattern is broad. Therefore, an angle deviation of canceler becomes not a serious matter. We fabricated two samples with the same parameters and confirmed their characteristics coincide. Thus, the fabricated error also does not a serious matter. A change in relative position between the target and the canceller is sensitive to the RCS reduction result. From Sect. 2, we must control relative phase differences in the 30° range to obtain a 10dB reduction. This corresponds to $\lambda_c/12$ deviation in δ at f_c. Such an order of alignment error may occur in an installation. If we seriously consider utilizing this method, an apparatus containing some alignment adjustable structure is desired.

5. Conclusion

Bandwidth enhancement by metasurfaces for RCS reduction based on scattering cancellation is studied. The metasurface is composed of the patch array on the substrate and designed by using the equivalent circuit model. The designed metasurface was fabricated and evaluated experimentally. Numerical and experimental evaluations verified that the metasurface enhances bandwidth of 10dB RCS reduction by 52% bandwidth ratio from 34% bandwidth ratio of metallic canceling scatterers. Therefore, effectiveness of the metasurface is confirmed.

References

[1] R.A. Shelby, D.R. Smith, and S. Schultz, "Experimental verification of a negative index of refraction," science, vol.292, no.5514, pp.77–79, 2001.

[2] D. Schurig, J.J. Mock, B.J. Justice, S.A. Cummer, J.B. Pendry, A.F. Starr, and D.R. Smith, "Metamaterial electromagnetic cloak at microwave frequencies," Science, vol.314, no.5801, pp.977–980, 2006.

[3] A. Alù, "Mantle cloak: Invisibility induced by a surface," physical review B, vol.80, no.24, 2009.

[4] J.C. Soric, P.Y. Chen, A. Kerkhoff, D. Rainwater, K. Melin, and A. Alù, "Demonstration of an ultralow profile cloak for scattering suppression of a finite-length rod in free space," New journal of Physics, vol.15, no.3, 2013.

[5] C.L. Holloway, E.F. Kuester, J.A. Gordon, J. O'Hara, J. Booth, and D.R. Smith, "An Overview of the Theory and Applications of Metasurfaces: The Two-Dimensional Equivalents of Metamaterials," IEEE Antennas Propag. Mag., vol.54, no.2, pp.10–35, April 2012.

[6] M. Paquay, J.-C. Iriarte, I.Ñ. Ederra, R. Gonzalo, and P. de Maagt, "Thin AMC Structure for Radar Cross-Section Reduction," IEEE Trans. Antennas Propag., vol.55, no.12, pp.3630–3638, Dec. 2007.

[7] Balanis, Constantine A. "4 Chapt. Linear Wire antenna" in Antenna theory: analysis and design, John wiley & sons, 2015.

[8] W. Chen, C.A. Balanis, and C.R. Birtcher, "Checkerboard EBG Surfaces for Wideband Radar Cross Section Reduction," IEEE Trans. Antennas and Propag., vol.63, no.6, pp.2636–2645, June 2015.

[9] S.H. Esmaeli and S.H. Sedighy, "Wideband radar cross-section reduction by AMC," Electronics Letters, vol.52, no.1, pp.70–71, 2016.

[10] J. Su, Y. Lu, J. Liu, Y. Yang, Z. Li, and J. Song, "A Novel Checkerboard Metasurface Based on Optimized Multielement Phase Cancellation for Superwideband RCS Reduction," IEEE Trans. Antennas Propag., vol.66, no.12, pp.7091–7099, Dec. 2018.

[11] J. Su, H. Yu, H. Yin, Q. Guo, Z. Xiao, and Z. Li, "Breaking the High-Frequency Limit and Bandwidth Expansion for Radar Cross-Section Reduction: A low-observable technology," IEEE Antennas Propag.

Mag., vol.63, no.6, pp.75–86, Dec. 2021.
[12] X. Liu, J. Gao, L. Xu, X. Cao, Y. Zhao, and S. Li, "A Coding Diffuse Metasurface for RCS Reduction," IEEE Antennas Wireless Propag. Lett., vol.16, pp.724–727, 2017.
[13] A.Y. Modi, C.A. Balanis, C.R. Birtcher, and H.N. Shaman, "New Class of RCS-Reduction Metasurfaces Based on Scattering Cancellation Using Array Theory," IEEE Trans. Antennas Propag., vol.67, no.1, pp.298–308, Jan. 2019.
[14] A.R. Varkani, Z.H. Firouzeh, and A.Z. Nezhad, "Design of a randomised arrangement AMC surfaces for RCS reduction based on equivalent circuit modelling," IET Microwaves Antennas and Propagation, vol.12, no.10, pp.1684–1690, 2018.
[15] R.J. Chaky, R.J. Beneck, E.B. Whiting, R.P. Jenkins, S.D. Campbell, and D.H. Werner, "Design of 3D Metamaterial Unit Cells for Broadband and Wide Field of View RCS Reduction," 2020 IEEE International Symposium on Antennas and Propagation and North American Radio Science Meeting, Montreal, QC, Canada, pp.1175–1176, 2020.
[16] R.J. Chaky, R.J. Beneck, S.D. Campbell, P.L. Werner, and D.H. Werner, "Design and Optimization of 3D Meta-Volumes for Complementary Phases Enabling Wide Field of View RCS Reduction," 2022 IEEE International Symposium on Antennas and Propagation and USNC-URSI Radio Science Meeting (AP-S/URSI), Denver, CO, USA, pp.1542–1543, 2022.
[17] A. Monti, J.C. Soric, A. Alù, A. Toscano, and F. Bilotti, "Anisotropic Mantle Cloaks for TM and TE Scattering Reduction," IEEE Trans. Antennas Propag., vol.63, no.4, pp.1775–1788, April 2015.
[18] M. Guo, W. Wang, J. Wang, and Y. Tong, "High Gain and Ultrabroadband RCS Reduction Fabry-Perot Antenna with Checkerboard Superstrate," 2020 IEEE International Symposium on Antennas and Propagation and North American Radio Science Meeting, Montreal, QC, Canada, pp.1259–1260, 2020.
[19] M. Guo, W. Wang, F. Hao, P. Huang, L. Gong, and X. Song, "Low RCS, Broadband Polarization Conversion Metasurface Antenna Based on Reactance Loading," IEEE Trans. Antennas Propag., vol.70, no.12, pp.11361–11374, Dec. 2022.
[20] Y. Tian, H. Gao, W. Yao, X. Huang, F. Peng, and L. Yu, "Out-of-Band RCS Reduction of HF/VHF Whip Antenna Using Curved AMC Structures," IEEE Trans. Antennas Propag., vol.70, no.11, pp.10086–10094, Nov. 2022.
[21] N. Nakamoto, T. Takahashi, T. Fukasawa, N. Yoneda, and H. Miyashita, "RCS Synthesis of Array Antenna With Circulators and Phase Shifters and Measurement Method for Deterministic RCS Reduction," IEEE Trans. Antennas Propag., vol.69, no.1, pp.135–145, Jan. 2021.
[22] N. Nakamoto, T. Takahashi, T. Fukasawa, and N. Yoneda, "RCS reduction of array antenna using circulator and phase shifter," 2017 IEEE Conference on Antenna Measurements & Applications (CAMA), Tsukuba, Japan, pp.190–193, 2017.
[23] N. Nakamoto, T. Takahashi, T. Nomura, M. Otsuka, and H. Miyashita, "A method to measure the antenna mode and structural mode for antenna RCS reduction using circulator and phase shifter," 2014 International Symposium on Antennas and Propagation Conference Proceedings, Kaohsiung, Taiwan, pp.21–22, 2014.
[24] M. Selvanayagam and G.V. Eleftheriades, "Experimental demonstration of active electromagnetic cloaking," Physical review X, vol.3, no.4, 2013.
[25] Nathan Marcuvitz, Waveguide handbook, no.21, Iet, 1951.
[26] O. Luukkonen, C. Simovski, G.É Granet, G. Goussetis, D. Lioubtchenko, A.V. Raisanen, and S.A. Tretyakov, "Simple and Accurate Analytical Model of Planar Grids and High-Impedance Surfaces Comprising Metal Strips or Patches," IEEE Trans. Antennas Propag., vol.56, no.6, pp.1624–1632, June 2008.
[27] R.F. Harrington, "Spherical Wave Functions," Time-Harmonic Electromagnetic Fields, IEEE, pp.264–316, 2001.
[28] R.F. Harrington, "Some Theorems and Concepts," Time-Harmonic Electromagnetic Fields, IEEE, pp.95–142, 2001.
[29] K. Zhao and L.E.R. Petersson, "A Robust Hybrid Electromagnetic Solver for Electrically Large Problems," 2018 IEEE International Conference on Computational Electromagnetics (ICCEM), Chengdu, China, pp.1–2, 2018.
[30] K. Zhao and L.E.R. Petersson, "Overview of Hybrid Solver in HFSS," 2018 IEEE International Symposium on Antennas and Propagation and USNC/URSI National Radio Science Meeting, Boston, MA, USA, pp.411–412, 2018.

Hiroshi Suenobu received the B.S. degree from Kochi University, M.S. and Ph.D. degrees from Nagoya University in 2011, 2013, and 2017, respectively. He joined Mitsubishi Electric Corporation, Tokyo in 2016. He has been engaged in research on the electromagnetic field and radar cross section analysis. He is currently with the Antenna Technology Department of the Information Technology Research and Development Center, Mitsubishi Electric Corporation. Dr. Suenobu received the Young Researcher's Award of IEICE Japan in 2018. He is a member of the IEEE.

Shin-ichi Yamamoto received the B.E., M.E. and D.E. degrees in electrical and electronic engineering from the Tokyo Institute of Technology, Tokyo, Japan, in 2001, 2003 and 2006, respectively. In 2006, he joined Mitsubishi Electric Corporation, Tokyo. Since then, he has been engaged in research and development of antennas for satellite communications and radar systems. He is currently with the Antenna Technology Department of the Information Technology Research and Development Center, Mitsubishi Electric Corporation. Dr. Yamammoto received the Young Researcher's Award of IEICE Japan in 2011. He is a member of the IEEE.

Michio Takikawa received B.E., M.E., and Ph.D. degrees from Nihon University in 2002, 2004 and 2016, respectively. In 2004, he joined Mitsubishi Electric Corporation, Tokyo. Since then, he has been engaged in research and development of antennas for satellite communications and radar systems. He is currently with the Defense System Division of the Defense & Space Systems Group, Mitsubishi Electric Corporation. Dr. Takikawa received the Young Researcher's Award of IEICE Japan in 2012. He is a member of the IEEE.

Naofumi Yoneda received the B.E., M.E., and Ph.D. degrees in electrical communication engineering from Tohoku University, Sendai, Japan, in 1988, 1990, and 1997, respectively. In 1990, he joined the Mitsubishi Electric Corporation, Kanagawa. He has been engaged in the research and development of antenna feeders and millimeter-wave circuits. He is currently a Chief Engineer of the Future Society Creation Lab., Information Technology Research and Development Center, Mitsubishi Electric Corporation. Dr. Yoneda is a member of the IEICE and served as a Vice President, Chair, Planning, Membership, and Finance Council Electronics Society of IEICE from 2013 to 2015. He received the Shinohara Memorial Young Investigators Award from the IEICE and Research and Development 100 Awards from Research and Development Magazine, in 1991 and 2005, respectively.